A STUDY OF COSMIC RAY VARIABILITY DURING A SOLAR MAGNETIC CYCLE (SOLAR CYCLES 23 AND 24)

Abstract

We investigated variations in Cosmic Ray (CR) intensities during Solar Cycles (SC) 23 and 24. Using data from the Mexico neutron monitor, solar wind parameters (speed, temperature, plasma density), geomagnetic indices (***Kp***, ***Dst***, ***ap***) from OMNI, and sunspot numbers from SISLO, we analyzed CR intensities during the ascending (ASC) and declining (DSC) phases of each cycle. Our analysis, using distribution plots and regression methods, showed higher CR intensities during the DSC phases compared to the ASC phases for both cycles. Additionally, average CR values were higher during SC 24 than SC 23. These variations are linked to differences in sunspot numbers, solar wind parameters, and geomagnetic indices, differences in magnetic transport across the Sun differ between the ASC and DSC phases, with SC 24 exhibiting weaker meridional flow compared to SC 23.

Keywords: Cosmic Rays, Method: Data Analysis, Method: Statistical, Sunspot Number

1 Introduction

Cosmic rays (CRs) are high-energy particles, primarily protons and atomic nuclei, that travel through space at nearly the speed of light. They originate from various sources, including the Sun, distant supernovae, and other energetic astrophysical phenomena. These particles can be detected on Earth or in space via their interactions with the atmosphere or detectors, where they create showers of secondary particles. Cosmic rays are classified based on their energy levels, ranging from a few MeV to more than 10^{20} eV (Rees & Sargent, 1968; Zweibel, 2013; Sparvoli & Martucci, 2022). Most CRs are protons, but they can also include heavier nuclei and electrons. Research suggests that they consist of 98% atomic nuclei and 2% electrons, with the nuclei including roughly 87% protons, 12% helium, and 1% heavier elements (Simpson 1983). Their study provides insights into high-energy processes in the universe, and their interactions help us understand astrophysical environments like the interstellar medium.

When cosmic rays (CRs) enter the Earth's atmosphere, they collide with atmospheric molecules, creating secondary particles in a phenomenon known as an air shower (Auger et al., 1939; Rossi, 1930). CRs are classified into two main types based on their origin: Galactic CRs, which originate from sources within our galaxy, such as supernovae and other stellar events (Vaclav, 2009; Ackermann et al., 2013), and extragalactic CRs (Sharma, 2008; Abramowski et al., 2016), which are believed to come from outside our galaxy, likely from extremely energetic events like active galactic nuclei, gamma-ray bursts, and magnetars (Vannoni et al., 2011; Hjorth & Bloom, 2012). The energy density of CRs averages around $1\text{eV}/\text{cm}^3$ of interstellar space

CRs can also be categorized by their energy levels; for example, low-energy CRs are trapped by the Earth's magnetic field and interact with the upper atmosphere, while high-energy CRs penetrate deeper into the atmosphere and are detectable by ground-based instruments (Anchordoqui et al., 2003; Abe et al., 2016). Studying cosmic rays allows scientists to gain insights into fundamental processes in the universe, such as the behavior of high-energy particles and the conditions in distant astrophysical objects.

Sunspots are large solar storms that are difficult to predict (Echer et al., 2004; Kane, 2006). They appear as dark areas on the surface of the Sun due to intense magnetic activity, inhibiting convection and leading to lower surface temperatures compared to surrounding areas. Their formation is linked to the Sun's magnetic field, as magnetic flux tubes rise through the solar surface due to buoyancy, creating localized areas of strong magnetic fields that become sunspots. These spots are important indicators of solar magnetic activity, which fluctuates over an approximately 11-year solar cycle (Solanki, 2003; Balogh, et al., 2014). Sunspots have effects beyond the Sun itself. They influence solar radiation and can impact space weather, including solar flares and coronal mass ejections. These solar phenomena can affect satellite communications, GPS systems, and power grids on Earth (Ruzmaikin, 2001; Solanki, 2002).

The number, coverage area, and intensity of sunspots vary in a cyclic pattern with a period of approximately 11 years, known as the solar cycle (SC). This cycle is monitored by counting sunspots, which are the most easily observed features of solar activity and have been tracked since the early 1600s (Hoyt & Schatten, 1979, 1998; Kane, 2006). Sunspots can appear as single, isolated dark central regions called umbrae

surrounded by a less dark pattern called penumbra, or in groups (Spiegel, 1994). At the core of the approximate 11-year cycle is the oscillating magnetic dynamo within the Sun, which changes approximately every 22 years (Denkmayr and Cugnon, 1997; Zhan et al., 2004; Xu et al., 2008). Sunspot cycles vary in size and length, making it challenging to describe their shape with a universal function (Layden et al., 1991; Conway, 1998). Many authors have attempted to describe these cycles as periodic phenomena, leading to a wealth of literature on the subject (Denkmayr and Cugnon, 1997; Hanslmeier et al., 1999; Zhan et al., 2004; Xu et al., 2008).

Numerous studies have examined the correlation between solar activities and the impact on cosmic ray (CR) intensity. Although CR intensity remains relatively steady outside the heliosphere, it varies during its journey through the heliosphere due to solar activities and changes in the interplanetary magnetic fields (Agrawal et al., 1993; Mavromichalaki et al., 1998; Bhattacharya and Roy, 2014). The fluctuations in CR intensity are mainly attributed to the outward release of solar outputs such as the solar wind, coronal mass ejections (CME), and solar flares. The solar wind influences the propagation of CRs, altering their paths and energies. In addition, changes in the configuration and strength of the heliospheric magnetic field can significantly modify CRs.

The Sun goes through a cycle called the Solar Cycle (SC) during which its magnetic field changes polarity. This cycle affects the level of solar modulation of CRs. The Sun's magnetic field drives activities such as sunspots, flares, prominence eruptions, and Coronal Mass Ejections (CMEs), which in turn influence Earth's upper atmosphere, magnetosphere, ionosphere, and near-Earth space environment. These solar disturbances also lead to fluctuations in CR flux, causing sudden increases known as Ground Level Enhancements (GLEs) and depressions called Forbush Decreases (FD). These variations show periodic changes including daily anisotropies, an 11-year solar cycle, 27-day Sun-rotation short-term variations, and rapid irregular changes (Forbush, 1946; Simpson, 1990; Jothe et al. 2010; Shrivastava et al. 2011; Gopalswamy et al., 2014; Okike et al. 2021; Okike and Alhassan 2021; Singh et al., 2023).

Over the years, several researchers (Cliver and Ling, 2001; Van Allen, 2000; Persai et al., 2015; Chaurasiya et al., 2023) have discovered a strong correlation between sunspot numbers (SSN) and various phenomena such as the modulation CR intensity, and CME (Onuchukwu, 2018). Therefore, it has been suggested that SSN could act as a proxy for long-term changes in the interplanetary magnetic field (IMF) over extended periods, consequently impacting CR intensity. According to Usoskin et al. (2005), the long-term variation in CR intensity demonstrates a significant sensitivity to SSN during periods of low solar activity and relative invariance during times of higher solar activity.

Over the years, many researchers (Cliver and Ling, 2001; Van Allen, 2000, Persai, et al., 2015; Chaurasiya et al., 2023) have found a strong correlation between sunspot numbers (SSN) and the modulation of CR intensity, SSN and coronal mass ejection (Onuchukwu, 2018) etc. Consequently, it has been proposed that SSN might serve as a proxy for long-term changes in the interplanetary magnetic field (IMF) over extended periods, thus affecting CR intensity. According to Usoskin et al. (2005), the long-term

variation in CR intensity shows a strong sensitivity to SSN during periods of low solar activity and relative invariance during times of higher solar activity.

This study seeks to investigate the fluctuation of CR intensity throughout the ascending (ASC)and declining (DSC) phases of SCs. CRs, composed of high-energy particles originating from sources beyond the solar system, exhibit varying levels of intensity influenced by the solar magnetic activity. During the ASC phase of solar cycles, solar magnetic activity gradually increases, reaching its peak at solar maximum, whereas during the DSC phase, solar activity diminishes towards solar minimum. The central questions guiding this research are outlined as follows:

- What is the temporal evolution of CR intensity during the ASC and DSC phases of SCs?
- Are there any correlations between CR intensity variations and solar activity such as sunspot number (SSN), and solar-terrestrial parameters (e.g. Solar Wind Speed (SWS), Solar Wind Temperature (SWT), Solar Wind Plasma Density (SWPD), Interplanetary Magnetic Field (IMF), geomagnetic activity indices like Dst, Kp and ap)?
- Are there potential differences in CR modulation mechanisms between the ASC and DSC phases of SCs?
- Identify any trends, periodicities, or anomalies in the CR intensity variations over solar magnetic cycles.

By addressing these issues, this study will help to advance our understanding of the complex interplay between solar activity and CR modulation, shedding light on the underlying mechanisms driving CR variations throughout different phases of SCs. Furthermore, the findings will contribute to enhancing space weather forecasting capabilities and mitigating potential risks associated with cosmic ray exposure in various domains.

2 Data:Data Description

The daily average sunspot data were obtained from the World Data Center SILSO, Royal Observatory of Belgium, Brussels (http://www.sidc.be/SILSO/). According to SILSO, SC 23 started in August 1996, lasted for 12.25 years reached its maximum in November 2001, and ended in November 2008. SC 24, stated in December 2008, reached its maximum in April 2014, lasting for a period of 11 years, ending in November 2019.

The CR data utilized in this study were sourced from the neutron monitor located at the central campus of the National Autonomous University of Mexico (UNAM), accessible through http://www.cosmicrays.unam.mx/. Managed by the Cosmic Ray Group of the Geophysical Institute at UNAM, Mexico City, the detector has operated since January 1, 1990. Positioned at 19.33 deg N latitude, 260.83 deg E longitude, and an altitude of 2274 m, with an effective cutoff rigidity of 8.2 GV, it serves as a reliable source for CR measurements. Fig 6 of Okike et al., (2020) illustrates that comparable data can be retrieved from the High-Resolution Neutron Monitor Database (NMDB) at http://www.nmdb.eu, as also noted by Mavromichalaki et al., (2011). Our study focused on daily pressure corrected CR data spanning from 1996 to 2019, encompassing

SCs 23 and 24. Utilizing averaged CR data offers advantages, notably in mitigating the effects of CR diurnal anisotropy, as discussed by Dumbovic et al., (2011) and Belov et al., (2018).

The studies by Gopalswamy et al. (2014), Lingri et al. (2016), and Okike & Umahi (2019), etc. have identified SC 23 as a significant period of heightened solar activity. Additionally, SC 23, known for its prolonged duration and intense solar activity, was followed by SC 24, which was characterized by a delayed and subdued maximum. Therefore, studying CR variations during these high active and subdued activity solar cycles, SC 23 and 24, provides us with a valuable opportunity.

The daily average solar wind parameters between 1996 and 2019 (like interplanetary magnetic field (IMF (nT)), solar wind temperature (SWT (K)), solar wind proton density (SWPD (N/cm^3), solar wind speed (SWS (km/s)), the geomagnetic activity indices - (Kp) (measured 3 hourly), Dst (measured 1 hourly), ap (measured 3 hourly)), were obtained from https://omniweb.gsfc.nasa.gov/.

We formed two subsamples for each SC: the ascending (ASC) phase and the declining (DSC) phase. According to SILSO, the ASC phase of SC 23 lasted from August 1996 to November 2001, while the DSC phase for SC 23 was from December 2011 to November 2012. For SC 24, the ASC phase was from December 2008 to April 2014, and the DSC phase was from May 2014 to November 2019.

3 Method of Analysis

We analyse the data by plotting the distribution (while checking for skewness, and kurtosis), such as histograms, make it easier to identify outliers or unusual observations that could impact the analysis. We also plot the time series graph. Time series analysis is a specific way of analysing a sequence of data points collected over an interval of time, and perform simple linear regression/correlation analysis (e.g. Fisher, 1915) to check for possible correlation between the parameters.

4 Results and Discussion

4.1 Time Series - Daily Variations

Figures 1-2 show the average daily variations of CR and SSN for the ASC and DSC phases of SC 23 and 24. The plot reveals higher CR intensity at the beginning and end of each SC, which is an in inverse correlation with the SSN, with overall higher CR intensity during SC 24 compared to SC 23 (Usoskin et al., 2002). The plots of the variation of daily average values of CR and SSN (see Figures 1-2) did not reveal clear trends due to rapid fluctuations. Therefore, we opted to plot the time series of variations of the monthly average values using the monthly average values.

Plotting monthly averages instead of daily or yearly averages offers several key advantages in data analysis and visualization. Firstly, monthly averaging effectively smooths out daily fluctuations and random noise, which may obscure significant trends when working with daily data. This reduction in data volatility allows for a clearer view of the underlying patterns, as noted in several studies on data smoothing techniques (Kass et al., 2018). Secondly, using monthly data facilitates the identification

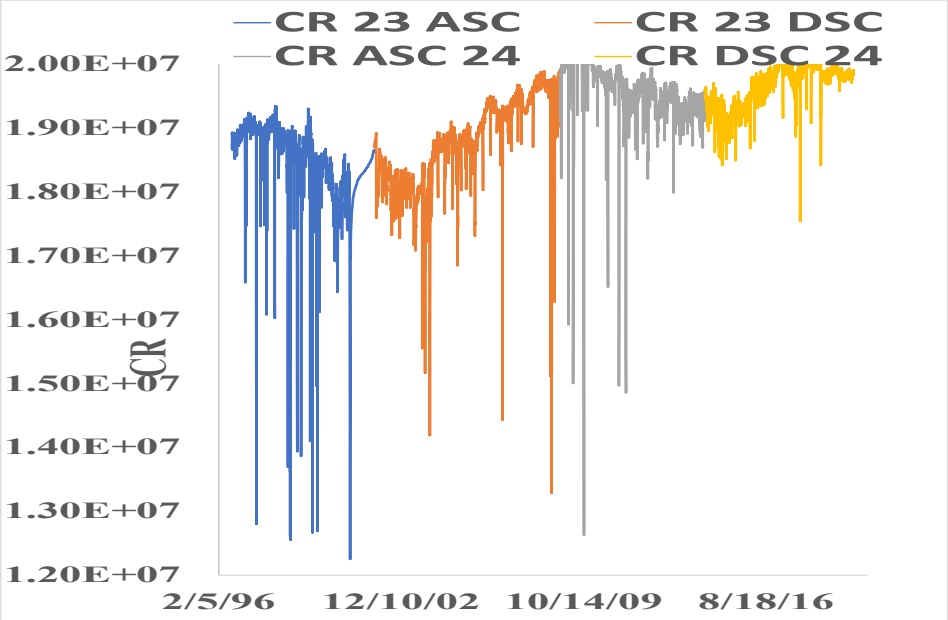

Fig. 1 Plot of Daily Variation of CR

of seasonal trends and cycles, which might not be apparent in yearly or daily datasets. Seasonal cycles are critical in climate and economic data, where monthly granularity helps uncover periodic patterns such as temperature fluctuations or market behaviors across different seasons (Mann, 2008). Furthermore, monthly averages strike an ideal balance between the detail of daily data and the broader perspective of yearly summaries, making it easier to manage and analyze large datasets. This balance is particularly beneficial in fields like finance and environmental science, where both detailed short-term changes and long-term trends are important (Rudebusch & Williams, 2009). Additionally, comparing monthly averages across years can highlight anomalies or unusual patterns that may go unnoticed when looking only at annual data, such as abnormal weather events or economic disruptions (Blazquez-Garcia et al., 2021). From a practical standpoint, monthly data sets are easier to handle, reducing the complexity involved in analyzing vast daily datasets. This simplification improves the efficiency of statistical tools and algorithms, making the analysis more feasible and less time-consuming (Jolliffe & Stephenson, 2012). Lastly, monthly averages enhance the clarity of visual representations, making it easier to communicate findings to a broader audience, including those without a technical background. By using monthly mean values, researchers can provide more robust and insightful analyses compared to daily

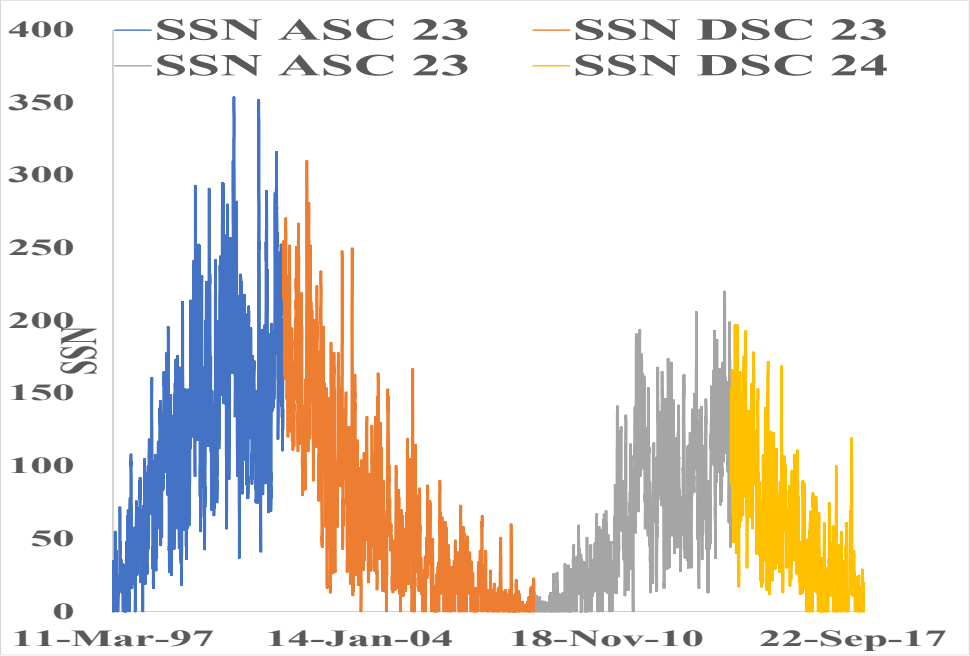

Fig. 2 Plot of Daily Variation of SSN

or yearly averages, capturing both trend consistency and anomalies in a manageable format (Tukey, 1977).

4.2 Monthly Average Time Series Plot

Figures 4-11 displays the time series plots of monthly average values for the ASC and DSC phases of SCs 23 and 24. These plots include cosmic ray (CR) intensity, sunspot number (SSN), solar-terrestrial parameters (interplanetary magnetic field (IMF), solar wind speed (SWS), solar wind temperature (SWT), solar wind plasma density (SWPD)), and geomagnetic activity indices (Kp, Dst, ap).

In SC 23, the intensity of CR was higher during the DSC phase (lowest monthly average values of (1.7×10^7 were recorded in July and November 2003) compared to the ASC phase with the lowest monthly average values recorded in October 1998 (1.8×10^7), July 2000 (1.8×10^7) and January 2001 (1.6×10^7). Similarly, in SC 24, CR intensity was higher during the DSC phase than the ASC phase. Overall, CR intensity was higher in SC 24 than in SC 23. The monthly average SSN values were higher in SC 23 than in SC 24. Generally, SSN values are higher during the ASC phases than the DSC phases for both cycles, although the DSC phases last longer than the ASC phases in both solar cycles. The double hump (peak-dip-peak) that characterize a SC

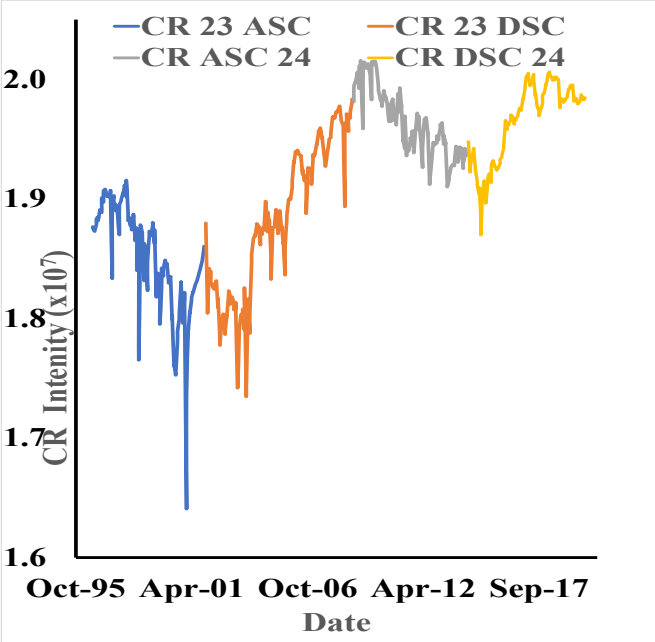

Fig. 3 Time Series Plots of the Monthly Average Values for ASC and DSC Phases of SC 23 and 24 for CR

(Ramesh, 2010, Onuchukwu 2018), occurred during the ASC phases of both SC. It is worth noting that CR values showed an inverse relationship with SSN values in each phase of SC 23 and 24. This finding is consistent with the results reported by various authors e.g. Mishra (2005), Mishra & Mishra (2016), and Chaurasiya et al. (2023), etc. The IMF displayed higher average monthly values in SC 23 than in SC 24. During SC 23, these IMF values were higher during the ASC phase than the DSC phase, whereas during SC 24, they were higher during the DSC phase than the ASC phase.

Solar wind parameters during SC 23 and SC 24 were compared as follows: during the ASC phases, SWS was higher during the ASC phase of SC 23 - average values in parentheses - (416.56 km/s) compared to SC 24 (387.98 km/s). SWT was significantly higher in SC 23 during the ASC phase (SC 23 $\times 10^4$ K; SC 24: 6.55 23 $\times 10^4$ K). SWPD was higher during the ASC phase of SC 23 (SC 23: 6.08 N/cm^3; SC 24: 5.07 N/cm^3). During the DSC phases: SWS was higher during the DSC phase of SC 23 (439.01 km/s) compared to SC 24 (417.47 km/s). SWT was higher during the DSC phase of SC 23 (SC 23: 9.64 23 $\times 10^4$ K; SC 24: 8.03 23 $\times 10^4$ K). SWPD was higher during the DSC phase of SC 24 compared to SC 23 (SC 23: 5.13 N/cm^3; SC 24: 6.21 N/cm^3). SWS was higher during SC 23 in both ASC and DSC phases compared to SC 24. SWT was higher during SC 23 in both ASC and DSC phases compared to SC 24. SWPD was higher in the ASC phase of SC 23 but higher in the DSC phase of SC 24. These

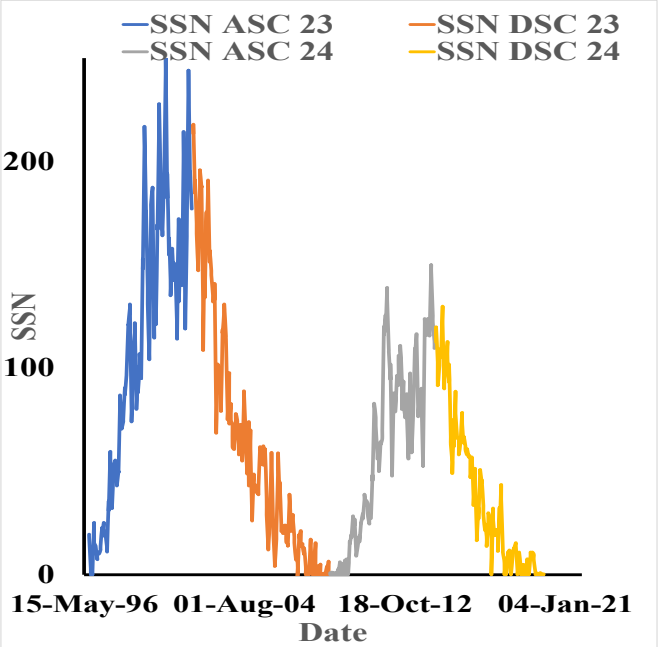

Fig. 4 Time Series Plots of the Monthly Average Values for ASC and DSC Phases of SC 23 and 24 for SSN

comparisons indicate that SC 23 generally experienced higher solar wind speeds and temperatures during both phases compared to SC 24, while solar wind plasma density showed varying trends, being higher in SC 23 during the ASC phase but higher in SC 24 during the DSC phase. These differences could reflect varying solar and heliospheric conditions between the two solar cycles. McComas et al., (2013) and Gopalswamy, et al. (2015), examine solar wind characteristics and geomagnetic activity during solar cycles 23 and 24. The authors find that the solar wind parameters, including speed, density, and temperature, were generally lower during solar cycle 24, which was the weakest cycle in over a century

For the geomagnetic activity indices, the Kp index monthly average values were higher during SC 23 than SC 24, they were generally lower during the ASC phase of SC 24 than other phases. The Dst index monthly average values were more negative during SC 23 than SC 24, indicating higher geomagnetic activity, they peaked negatively during high SSN, indicating increased geomagnetic activity during high solar activity. The ap index average monthly values were higher during SC 23 than SC 24, indicating higher geomagnetic activity, and generally, peaks during high SSN values, suggesting more geomagnetic activity during periods of high solar activity. This comprehensive analysis reveals that SC 23 exhibited higher geomagnetic activity, CR intensity differences, and solar-terrestrial parameter variations compared to SC 24, with distinct

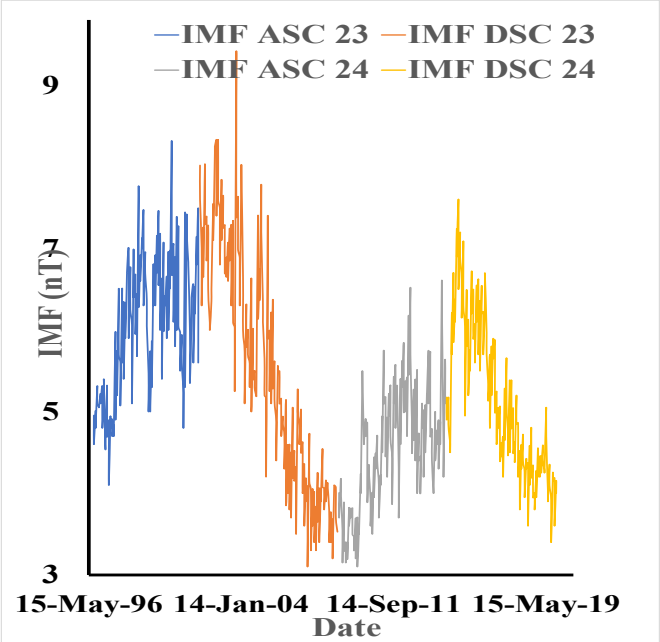

Fig. 5 Time Series Plots of the Monthly Average Values for ASC and DSC Phases of SC 23 and 24 for IMF

patterns observed between the ASC and DSC phases in each cycle.Gonzalez et al. (2011) and Tsurutani et al. (2014) showed that geomagnetic indices such as Dst and Kp were generally higher during solar cycle 23 than 24. The study attributes this to the higher solar activity and stronger solar wind parameters during cycle 23 compared to the weaker cycle 24. Kilpua et al. (2015) and Richardson (2013) highlight that during the ascending phase of solar cycle 23, there were more frequent and intense geomagnetic storms compared to solar cycle 24, due to stronger solar wind streams and more frequent CMEs.

Table 1 presents the estimated median and mean values along with the associated standard errors for various parameters analysed.

- CR Intensity average values showed similar values during ASC and DSC phases of each SC, and were higher during SC 24 than SC 23.
- SSN average values indicate higher during the ASC phase than the DSC phase for both SCs, and were higher during SC 23 than SC 24.
- IMF average values showed higher values during the ASC phase of SC 23, and lowest during the ASC phase of SC 24.
- SWS and SWT average values were higher during the DSC phase of each SC than during the ASC phase, they were also higher during SC 23 than SC 24.

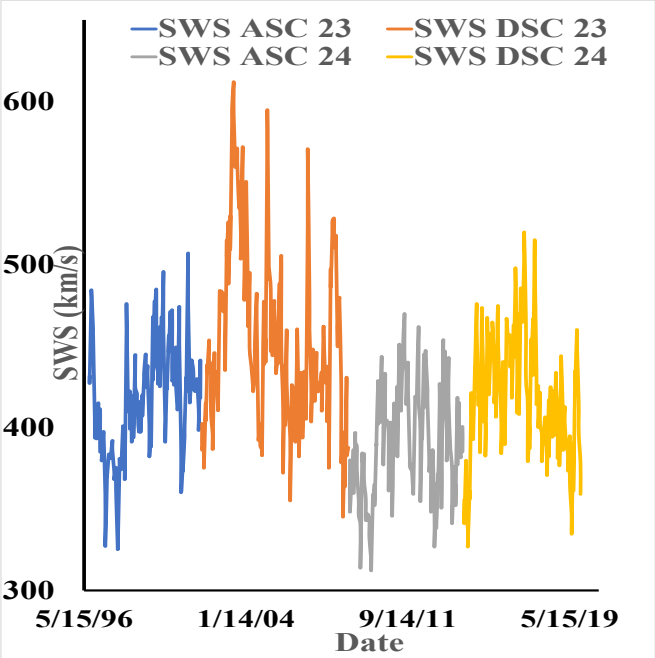

Fig. 6 Time Series Plots of the Monthly Average Values for ASC and DSC Phases of SC 23 and 24 for SWS

- SWPD average values were higher during the ASC phase than the DSC phase. SWPD values did not follow any specific trend relative to the SSN cycle.
- Geomagnetic Indices (Kp, Dst, ap) average values generally have higher positive or negative values during SC 23 than SC 24, also, they average values indicate that high geomagnetic activities correlate with high solar activities, as measured by SSN.

4.3 Monthly Average Distribution Plots

The plots of the monthly average distribution for CR, SSN, IMF, solar wind parameters (SWS, SWT, SWPD) and geomagnetic activity indices (Kp, Dst, ap) for the ASC and the DSC phases of SC 23 and 24 are shown in Figures 12-16. the kurtosis and the skewness of the distribution are shown in Table 2 for each phase.

The analysis of CR intensity during the ASC and DSC phases of SCs 23 and 24 reveals distinct statistical characteristics in their distributions. For the ASC phase of SC 23, the distribution is negatively skewed and leptokurtic, indicating a long left tail and a higher propensity for extreme values due to heavier tails and a sharper peak compared to a normal distribution. This suggests greater variability and more pronounced CR intensity fluctuations during this period. In contrast, the DSC phase of SC 23 shows a slightly negatively skewed but more symmetric and platykurtic distribution,

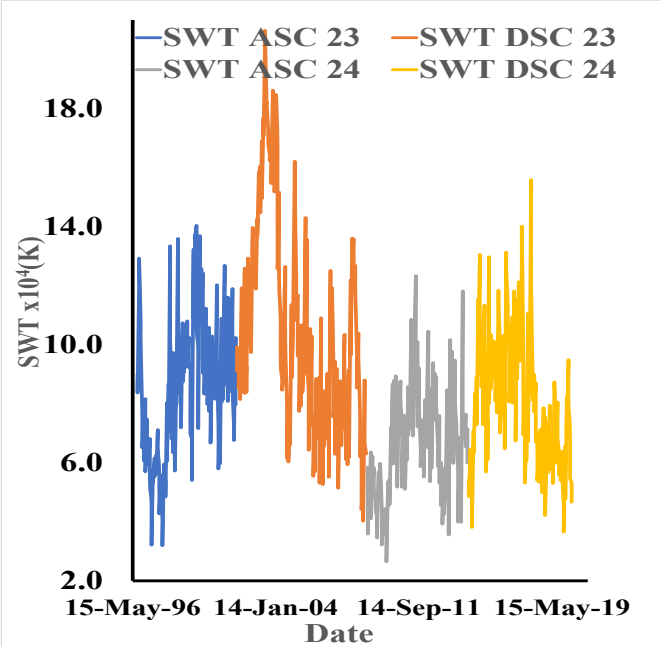

Fig. 7 Time Series Plots of the Monthly Average Values for ASC and DSC Phases of SC 23 and 24 for SWT

implying fewer extreme values, a more uniform spread, and a flatter peak, signaling more stability in CR intensity during this phase. For SC 24, the ASC phase presents a slightly positively skewed and platykurtic distribution, meaning a smaller right tail with fewer extreme values and a more balanced, evenly spread pattern. Meanwhile, the DSC phase of SC 24 is negatively skewed and platykurtic, indicating a longer left tail with fewer outliers and a generally uniform spread of CR intensities. These findings show that the ASC phase of SC 24 has a nearly symmetric distribution, with a slight tendency toward higher values, whereas the DSC phase has lower values with fewer extreme variations but remains evenly distributed. This comparison between SC 23 and SC 24 highlights the differences in monthly average CR intensity variations, particularly in how solar modulation, influenced by solar wind conditions and magnetic fields, impacts cosmic ray propagation differently during the ASC and DSC phases (Moraal & McCracken, 2012; Potgieter, 2013; Ahluwalia & Ygbuhay, 2014; Aslam & Badruddin, 2015). Further studies by Heber et al. (2009), Kuwabara et al. (2009), and Gieseler et al. (2017) explain that solar magnetic field changes, solar wind speed, and the tilt angle of the heliospheric current sheet during different solar cycle phases affect cosmic ray modulation. The reversal of the Sun's magnetic field near the solar cycle peak significantly influences cosmic ray propagation during the ASC and DSC phases, leading to the observed differences in CR distribution and intensity.

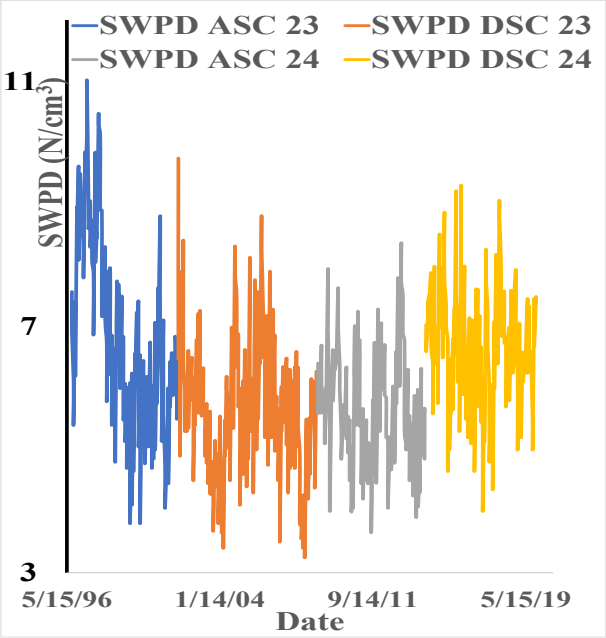

Fig. 8 Time Series Plots of the Monthly Average Values for ASC and DSC Phases of SC 23 and 24 for SWPD

The SSN distribution in different SC 23 and 24 phases show that ASC phases are almost symmetrical with a slight right skew, suggesting balanced distributions around the mean. The distributions are platykurtic, especially in SC 24, indicating fewer extreme values. The DSC phases of both cycles are moderately right-skewed, indicating a predominance of lower values with a tendency towards higher values. Overall, the ASC phases of both cycles show nearly symmetrical and flatter distributions, while the DSC phases are moderately right-skewed with tail behaviors closer to normal but slightly platykurtic in SC 24. During the DSC phase of a SC, the SSNs typically decline gradually. This extended period of lower sunspot numbers would mean more frequent occurrences of low values. The DSC phases of SCs are right-skewed due to extended period lower SSN during the declining phase. Research by Abha et al. (2024) discusses how sunspot group dynamics, including flare activity and magnetic complexity, differ across phases and SCs, further explaining the variability in SSN distributions. Additional studies, such as those by Hathaway and Upton (2014) and Iwok (2011), also corroborate the distinct distribution behaviors seen between the ASC and DSC phases of SCs 23 and 24.

The distribution of the IMF for SC 24, as depicted in Figure 13, shows a slightly right-skewed and moderately platykurtic ASC Phase, indicating mild asymmetry with

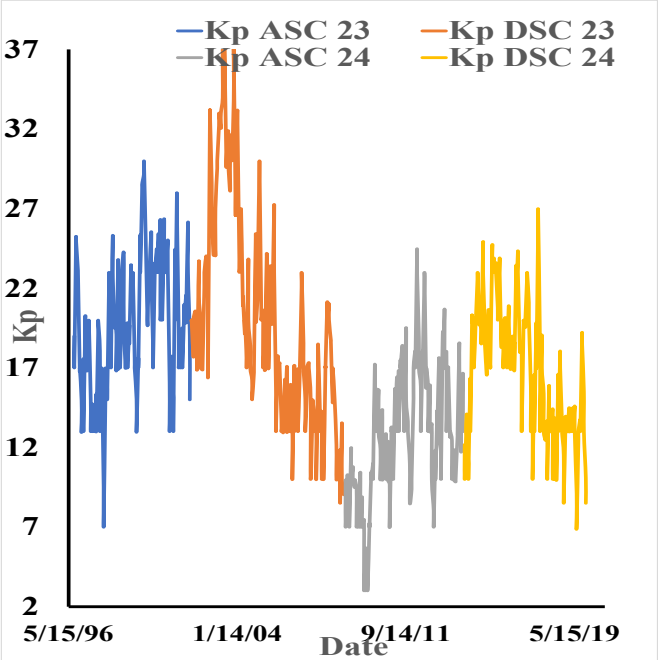

Fig. 9 Time Series Plots of the Monthly Average Values for ASC and DSC Phases of SC 23 and 24 for Kp

more frequent lower values and a somewhat flatter shape compared to a normal distribution. The DSC Phase is moderately right-skewed and slightly platykurtic, displaying more noticeable asymmetry with more frequent lower values and a longer tail towards higher values. Both ASC phases (SC 23 and SC 24) exhibit slight right skewness, with SC 23 being almost symmetrical and platykurtic, indicating flatter distributions with fewer extreme values. Both DSC phases show right skewness, with SC 24 having a higher skewness value, indicating more pronounced asymmetry. Both phases are platykurtic, with SC 23 being more so, indicating fewer extreme values than SC 24. This analysis highlights the differences in distribution shapes between the ASC and DSC phases of SCs 23 and 24, particularly in terms of symmetry and tail behavior. The Sun is the source of IMF, any changes in the Sun magnetic field patterns will manifest in the recorded values of IMF. Upton et al., (2021), reported variations in the meridional flow, which were more pronounced in SC 23 than in the weaker SC 24.

The SWS distribution during the ASC phase of SC 23 is almost perfectly symmetrical, while the DSC phase of SC 23 is moderately skewed to the right. The ASC phase of solar cycle 24 also shows an almost perfectly symmetrical distribution, while the DSC phase has a slight right skew. Both ASC phases are close to mesokurtic, while the DSC phases are slightly platykurtic. This comparison highlights the differences in symmetry and tail behavior between the ASC and DSC phases of solar cycles 23 and

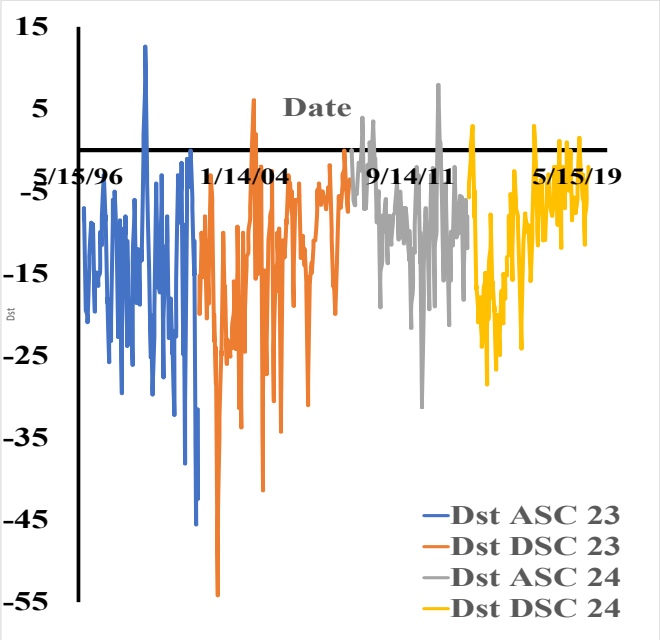

Fig. 10 Time Series Plots of the Monthly Average Values for ASC and DSC Phases of SC 23 and 24 for *Dst*

24, indicating variations in SWS distribution characteristics. Studies on the statistical distribution of CME and solar wind speeds provide insight into how these phases exhibit distinct patterns in terms of symmetry and kurtosis, with ASC phases being closer to mesokurtic and DSC phases slightly platykurtic (Zhang et al., 2021; Echer et al., 2023; Mishra et al., 2024), these conclusions were similar to ours.

The analysis indicates that for the SC 23 ASC phase, the SWT distribution displays a slight right skew, signifying a mild asymmetry with a tendency towards higher values. The distribution is also platykurtic, indicating that it is flatter than a normal distribution with fewer extreme values. In the case of the SC 23 DSC phase, the distribution is moderately skewed to the right, suggesting more frequent lower values and a tail extending towards higher values. It is also slightly platykurtic, signifying that it is somewhat flatter than a normal distribution. Moreover, the ASC phase of SC 24 exhibited a distribution that is more skewed to the right than the ASC phase of SC 23, demonstrating a greater tendency towards higher values, and slight platykurtic characteristics, close to mesokurtic, indicating tails similar to a normal distribution but slightly flatter. Similarly, the DSC phase of SC 24 distribution is moderately skewed to the right, indicating an asymmetry with more frequent lower values and a tail towards higher values. It is slightly platykurtic, indicating that it is flatter than a normal distribution but closer to mesokurtic compared to the DSC phase of SC 23. In

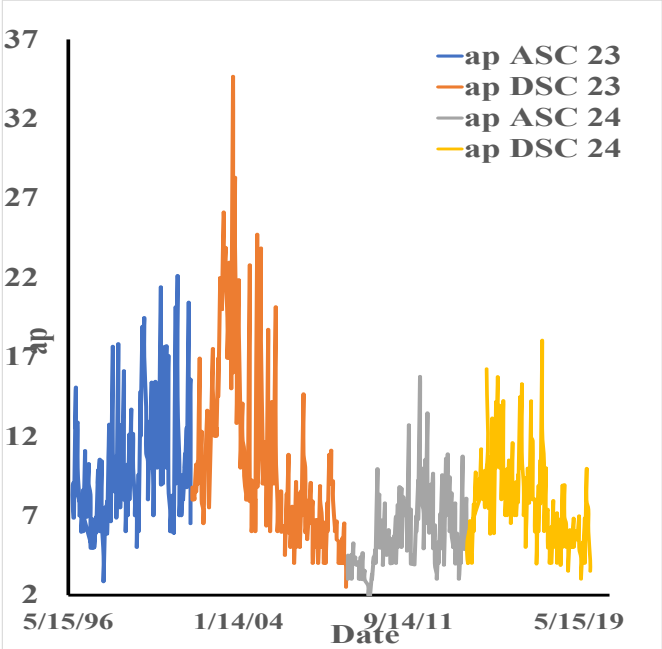

Fig. 11 Time Series Plots of the Monthly Average Values for ASC and DSC Phases of SC 23 and 24 for *ap*)

summary, during the ASC phases, both cycles have slightly right-skewed distributions, with SC 24 being more skewed and less flat (less platykurtic) than SC 23. During the DSC phases, both cycles exhibit moderate right skewness, with SC 23 having a more pronounced skew and flatter distribution compared to SC 24. This comparison emphasizes symmetry and tail behavior between the ASC and DSC phases of SCs 23 and 24, revealing differences in the distribution of SWT. The works by White et al., (2011), Gopalswamy et al. (2012), Zhang et al., (2021) and other researchers used microwave observations and magnetic field data to supports the idea that the solar wind properties, including SWT, display different behaviors during the ASC and DSC phases of solar cycles 23 and 24. They observed notable differences in solar activity during these phases, including the presence of skewness in solar wind parameters due to solar events CMEs, which are more frequent in the ASC phase, contributing to the right skew. Further, research examining solar minimum periods between cycles 23 and 24 noted variations in solar irradiance and solar wind characteristics, which ties into your description of kurtosis, where distributions tend to be flatter during quieter periods and exhibit more pronounced tails during higher solar activity.

The SWPD distribution for the ASC phase of SC 23 is moderately skewed to the right, with a tendency for more frequent lower values and a tail extending towards higher values. The DSC phase of SC 23 shows similar right skewness and is also

Table 1 Table of Monthly Average Values Estimated For CR, SSN, IMF, SWS, SWT, SWPD, $Kp, Dst.ap$ for SCs 23 and 24

Parameter	ASC 23	DSC 23	ASC 24	DSC 24
		Median		
CR ($\times 10^7$)	1.86	1.88	1.96	1.98
SSN	115.74	46.53	60.61	24.25
IMF (nT)	6.23	5.51	4.73	5.08
SWS (km/s)	416.56	439.01	387.98	417.47
SWT ($\times 10^4$ K)	8.53	9.64	6.55	8.03
SWPD (N/cm^3)	6.08	5.13	5.07	6.21
Kp	19.58	18.51	13.01	17.01
Dst	-14.01	-11.37	-7.42	-8.13
ap	9.32	8.58	5.01	7.62
		Mean with σ		
CR ($\times 10^7$)	1.85±0.36	1.88±0.53	1.96±0.24	1.97±0.28
SSN	109.40±57.11	60.41±45.12	60.27±38.55	37.04±30.49
IMF (nT)	6.24±0.73	5.73±1.25	4.76±0.63	5.53±0.81
SWS (km/s)	416.23±28.23	453.75±44.81	390.58±28.53	419.48±31.39
SWT ($\times 10^4$ K)	8.57±1.99	5.18±0.91	5.16±0.76	6.19±0.79
SWPD (N/cm^3)	6.33±1.29	5.18±0.91	5.16±0.76	6.19±0.79
Kp	19.74±3.55	19.96±5.42	12.72±3.27	16.80±3.63
Dst	-14.35±7.57	-13.33±7.39	-8.10±4.65	-9.75±5.96
ap	10.28±3.16	10.15±4.41	5.86±1.98	7.94±2.32

Table 2 Table of Values for the Estimated Skewness (S) and Kurtosis (K) for the Distribution Plots

	ASC 23	ASC 23	DSC 23	DSC 23	ASC 24	ASC 24	DSC 24	DSC 24
	S	K	S	K	S	K	S	K
CR	-1.24	2.99	-0.24	-0.98	0.23	-0.96	-0.76	-0.53
SSN	0.03	-1.00	0.99	0.05	0.08	-1.29	0.82	-0.44
IMF	0.03	-0.80	0.28	-0.99	0.21	-0.37	0.49	-0.72
SWS	0.06	-0.03	0.75	-0.07	0.04	-0.64	0.13	-0.18
SWT	0.18	-0.51	0.69	-0.19	0.39	-0.11	0.55	-0.04
SWPD	0.43	-0.39	0.46	0.46	0.38	-0.15	-0.03	0.06
Kp	-0.02	-0.28	0.68	-0.26	0.23	0.11	0.06	-0.75
Dst	-1.06	1.70	-0.73	0.60	-0.60	1.82	-0.47	-0.56
ap	0.93	0.35	1.41	1.86	1.18	1.80	0.87	0.76

leptokurtic, indicating a more peaked distribution with heavier tails. The ASC phase of SC 24 has a slightly skewed right distribution, while the DSC phase of SC 24 is almost symmetrical. In summary, both cycles show moderate right skewness during their ASC phases, but the DSC phases exhibit different distribution shapes, with SC 23 being leptokurtic and SC 24 being closer to mesokurtic.

The analysis of the distributions of the Kp, Dst, and ap indices during the SC 23 and 24 phases can be supported by several studies that analyze the geomagnetic and solar activity. For instance, the Kp index distribution during SC 23's ASC and DSC phases shows differences in symmetry and tail behavior, which correlate with the frequency and intensity of geomagnetic events. Research reveals that during the ASC of SC 23, the distribution is nearly symmetrical and slightly platykurtic, indicating a flatter-than-normal spread with fewer extreme values (Rangarajan & Lyemori, 1997).

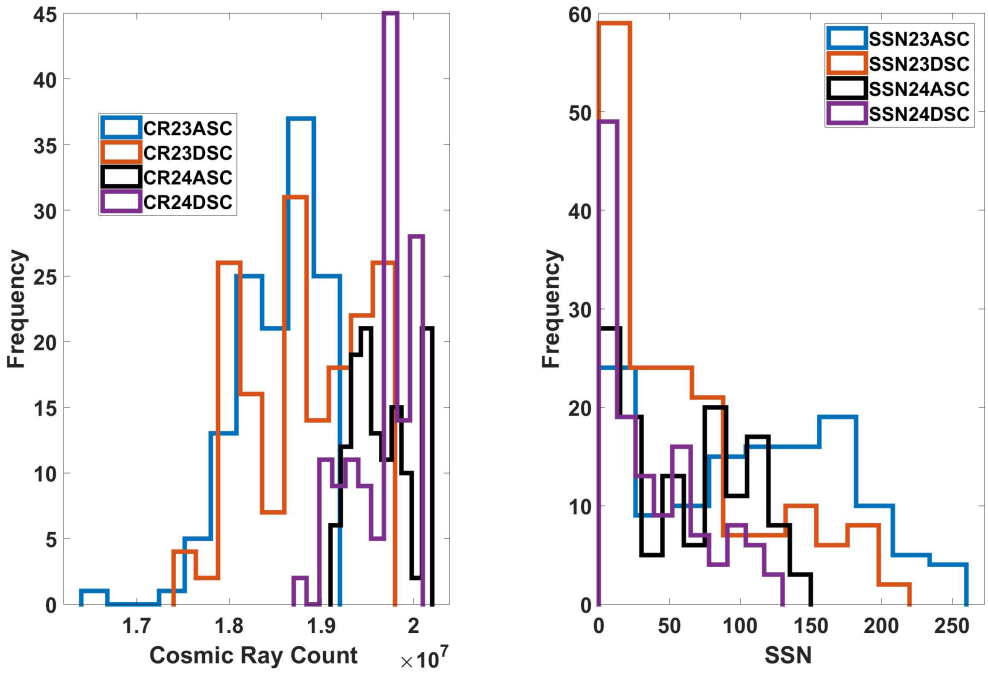

Fig. 12 Plots of the Monthly Average Distributions of ASC and DSC Phases of SC 23 and 24 for CR, SSN)

Similarly, during SC 23's DSC phase, a moderate right skew is observed, highlighting a tail towards higher values, while SC 24 shows a similar but less pronounced distribution.

For the *Dst* index, studies indicate that during the ASC phase of SC 23, a negative skewness with leptokurtic characteristics is present, suggesting extreme values and heavy tails, signifying intense geomagnetic storms. This pattern is less extreme in SC 24, where fewer negative extreme values and a more normal-like distribution are observed, particularly in the DSC phase.

Lastly, the *ap* index distribution shows significant differences in right skewness and kurtosis between the two solar cycles. During SC 23's DSC phase, a pronounced right skew and leptokurtic behavior highlight frequent extreme values and a long tail towards higher values. In contrast, SC 24 exhibits less extreme but still noticeable right skewness. These variations in skewness and kurtosis provide insights into the intensity and frequency of geomagnetic storms, with SC 23 showing more extreme behavior than SC 24, especially during the DSC phases. These observations are crucial for understanding space weather patterns and the impact of solar activity on geomagnetic indices across different solar cycles.

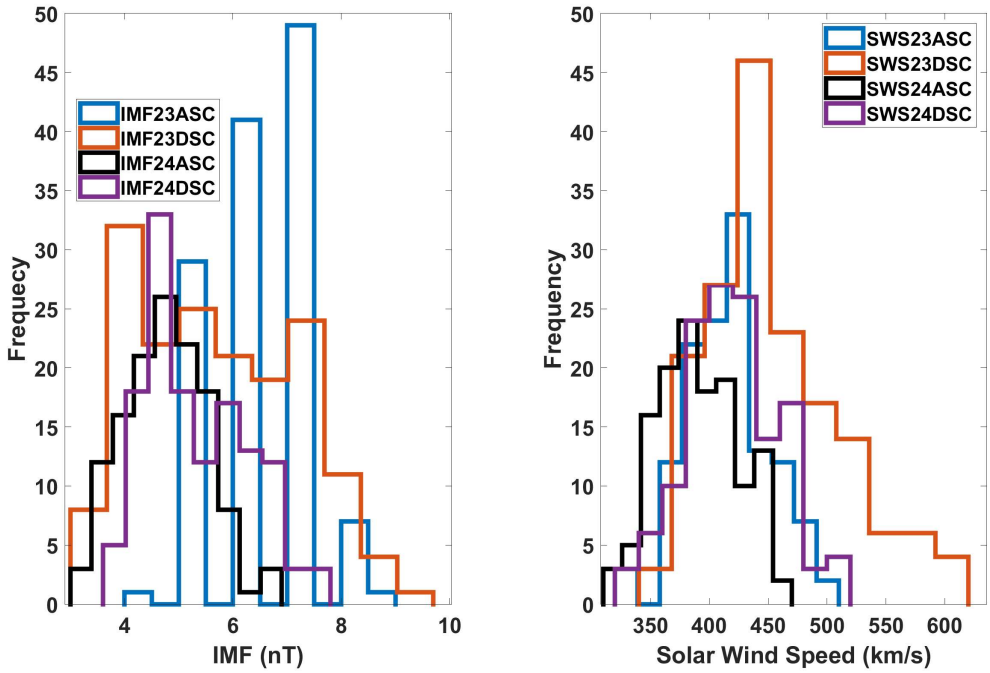

Fig. 13 Plots of the Monthly Average Distributions of ASC and DSC Phases of SC 23 and 24 for IMF, SWS

Table 3 display the correlation coefficients and Table 4, the results of $\log - \log$ fit to the monthly average values of the studied parameters, while the $\log - \log$ plots of CR intensity against SSN, IMF, SWS, SWT, SWPD and the geomagnetic indices (Kp, Dst, ap) are shown in Figure 4 These results suggest for CR and SSN that while the overall relationship patterns are consistent (negative correlations) for both phases of SC 23 and 24, SC 23 exhibited a slightly stronger and more pronounced relationship between CRs and SSNs compared to SC 24. During the ASC phase of SC 23 and SC 24, Table 3 shows that both have a similar slope, indicating a similar relationship between CR and SSN. In the DSC phase, SC 23's slope is slightly steeper than SC 24's, suggesting a stronger negative correlation between CR and SSN. Despite these differences, the intercepts are very close, suggesting similar overall cosmic ray intensity levels across both solar cycles.

The linear fit indicates that the relationship between CR intensity and IMF is stronger in SC 23 compared to SC 24. The CR intensity is more sensitive to changes in IMF during the ASC and DSC phases of SC 23, with the steepest decline observed during the DSC phase. The baseline CR intensity remains fairly consistent across the different phases and cycles.

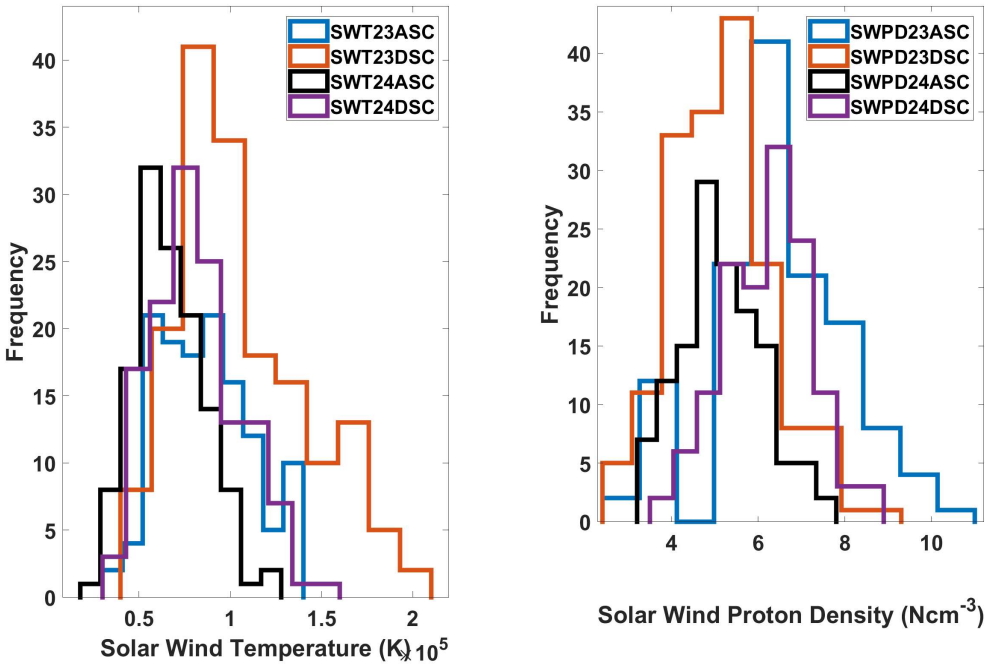

Fig. 14 Plots of the Monthly Average Distributions of ASC and DSC Phases of SC 23 and 24 for Solar Wind Parameters (SWT, SWPD)

The comparison of linear fits between CR intensity and SWT during the ASC and DSC phases of SCs 23 and 24 reveals that both SCs have the same slope of -0.03 with the same uncertainty (0.01). SC 23 has a steeper slope (-0.07) compared to SC 24 (-0.02) during the DSC phase, indicating a much stronger inverse relationship. The DSC phase in SC 23 shows a particularly strong inverse relationship (-0.07) between CR and SWT, suggesting that CR intensity is more sensitive to changes in SWT during this phase. The ASC phases of both SCs have identical slopes and very similar intercepts, indicating a consistent inverse relationship between CR and SWT. In summary, the relationship between cosmic ray intensity and solar wind turbulence shows a significantly stronger inverse correlation during the DSC phase of SC 23 compared to SC 24, while the ASC phases are remarkably consistent across both cycles.

The relationships between CR intensity and SWPD during the ASC and DSC phases of SCs 23 and 24 show that the ASC phase of SC 23 indicates a moderate positive correlation between CR and SWPD. As SWPD increases, CR increases moderately. During the DSC of SC 23, the result shows a weak positive correlation, and the CR is almost independent of SWPD during this phase. The ASC phase of SC 24 indicates a slight positive correlation, while the DSC phase of SC 24 shows a slight negative correlation. The intercepts are similar across all phases and cycles, with slight

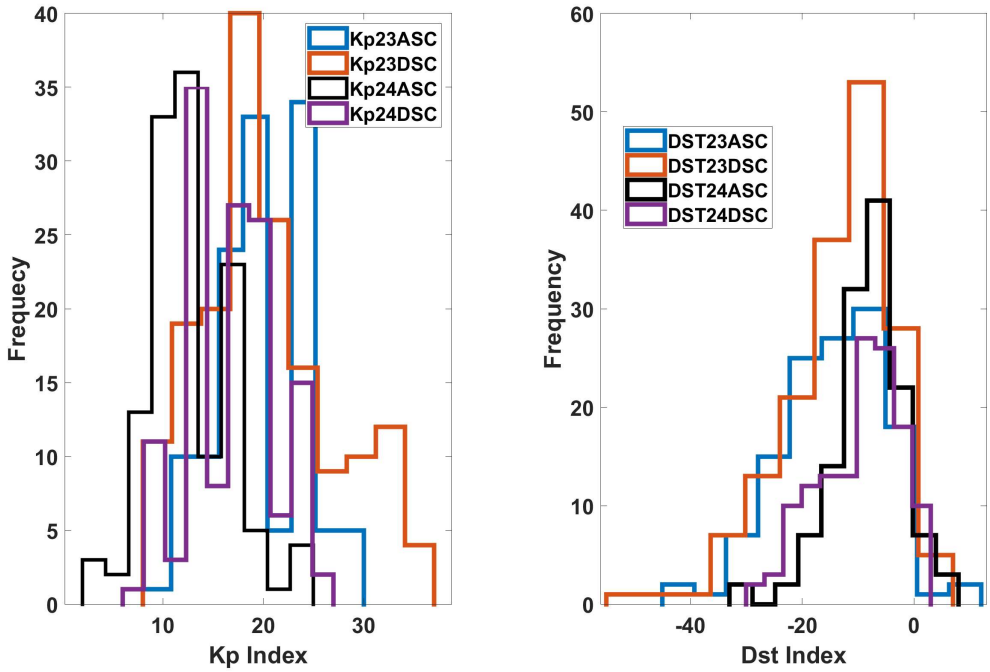

Fig. 15 Plots of the Monthly Average Distributions of ASC and DSC Phases of SC 23 and 24 for Geomagnetic Activity Indices (Kp, Dst)

variations. The ASC phase of SC 23 shows the highest sensitivity to SWPD, followed by the ASC phase of SC 24. Both DSC phases show very little sensitivity, with SC 24's DSC phase even showing a slight negative correlation. Overall, the ASC phases are more sensitive to changes in SWPD than the DSC phases in both solar cycles.

The relationships between CR intensity and SWS during the ASC and DSC phases of SCs 23 and 24, given by the result of the linear fits, indicate a moderate negative correlation between CR and SWS during the ASC phase of SC 23. As SWS increases, CR decreases moderately. The DSC phase of SC 23 shows a slightly stronger negative correlation than the ASC phase. The ASC phase of SC 24 displays a weaker negative correlation compared to SC 23. As SWS increases, CR decreases, but less steeply. The DSC phase of SC 24 shows a very weak negative correlation, almost negligible. The intercepts are higher for SC 23 compared to SC 24, indicating higher baseline CR levels in SC 23. In conclusion, SC 23 shows a stronger and more consistent negative relationship between CR and SWS across both phases, whereas SC 24 shows a weaker and phase-dependent relationship. The relationship between CR intensity and the Kp index (a measure of geomagnetic activity) during the ASC and DSC phases of SCs 23 and 24 exhibits significant variations. In the ASC phase of SC 23, a moderate negative correlation between CR and Kp is observed, while during the DSC phase, it shows

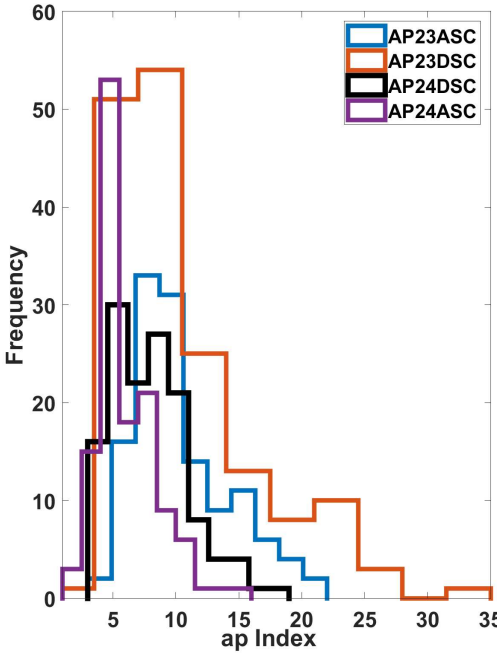

Fig. 16 Plots of the Monthly Average Distributions of ASC and DSC Phases of SC 23 and 24 for *ap*)

Table 3 Correlation Coefficient for the Different phases of SC 23 and 24 Estimated between the studied parameters

	ASC 23	DSC 23	ASC 24	DSC 24
	r	r	r	r
CR/SSN	-0.8	-0.8	-0.7	-0.7
CR/IMF	-0.4	-0.9	-0.7	-0.8
CR/SWT	-0.4	-0.7	-0.5	-0.3
CR/SWPD	0.5	0.0	0.3	-0.1
CR/SWS	-0.4	-0.5	-0.5	-0.1
CR/Kp	-0.4	-0.8	-0.7	-0.5
CR/Dst	0.1	0.5	0.5	0.6
CR/ap	-0.3	-0.6	-0.5	-0.3

a stronger negative correlation. The ASC phase of SC 24 displays a weaker negative correlation compared to SC 23. In the DSC phase of SC 24, the negative correlation is similar to the ASC phase. The DSC phase of SC 23 shows the strongest negative correlation, followed by the ASC phase of SC 23. Both phases of SC 24 show similar and weaker negative correlations. Overall, SC 23 shows a stronger and more variable negative relationship between CR and Kp, while SC 24 shows a consistent but weaker negative relationship in both phases.

Table 4 log − log Linear Regression to Fit studied parameters

SC	ASC	DSC
SC23	log CR= $-(0.01 \pm 0.01)$ log SSN $+\log 7.29$	log CR= $-(0.02 \pm 0.01)$ log SSN $+\log 7.31$
SC24	log CR= $-(0.01 \pm 0.01)$ log SSN $+\log 7.31$	logCR= $-(0.01 \pm 0.01)$ log SSN $+\log 7.31$
SC23	log CR= $-(0.07 \pm 0.01)$ log IMF $+\log 7.33$	log CR= $-(0.11 \pm 0.01)$ log IMF $+\log 7.36$
SC24	log CR= $-(0.06 \pm 0.01)$ log IMF $+\log 7.34$	logCR= $-(0.07 \pm 0.01)$ log IMF $+\log 7.35$
SC23	log CR= $-(0.03 \pm 0.01)$ log SWT $+\log 7.43$	log CR= $-(0.07 \pm 0.01)$ log SWT $+\log 7.61$
SC24	log CR= $-(0.03 \pm 0.01)$ log SWT $+\log 7.42$	log CR= $-(0.02 \pm 0.01)$ log SWT $+\log 7.37$
SC23	log CR= (0.04 ± 0.01) log SWPD $+\log 7.23$	log CR= (0.01 ± 0.01) log SWPD $+\log 7.28$
SC24	log CR= (0.02 ± 0.01) log SWPD $+\log 7.28$	logCR= $-(0.01 \pm 0.01)$ log SWPD $+\log 7.31$
SC23	log CR= $-(0.11 \pm 0.01)$ log SWS $+\log 7.56$	logCR= $-(0.13 \pm 0.01)$ log SWS $+\log 7.62$
SC24	log CR= $-(0.08 \pm 0.01)$ log SWS $+\log 7.51$	logCR= $-(0.01 \pm 0.01)$ log SWS $+\log 7.33$
SC23	log CR= $-(0.04 \pm 0.01)$ log Kp $+\log 7.32$	log CR= $-(0.08 \pm 0.01)$ log Kp $+\log 7.38$
SC24	log CR= $-(0.03 \pm 0.01)$ log $Kp + \log 7.32$	logCR= $-(0.03 \pm 0.01)$ log $Kp + \log 7.33$
SC23	log CR= (0.01 ± 0.01) log $\lvert Dst \rvert + \log 7.27$	log CR= $-(0.02 \pm 0.01)$ log $\lvert Dst \rvert + \log 7.31$
SC24	log CR= $-(0.01 \pm 0.01)$ log $\lvert Dst \rvert + \log 7.31$	logCR= $-(0.01 \pm 0.01)$ log $\lvert Dst \rvert + \log 7.31$
SC23	log CR= $-(0.02 \pm 0.01)$ log ap $+\log 7.29$	logCR= $-(0.05 \pm 0.01)$ log ap $+\log 7.32$
SC24	log CR= $-(0.02 \pm 0.01)$ log ap $+\log 7.31$	log CR= $-(0.02 \pm 0.01)$ log ap $+\log 7.31$

The relationship between CR intensity and the Dst index (which measures geomagnetic activity related to the ring current) during the ASC and DSC phases of SCs 23 and 24 is given in Table 4 (we use the absolute value of Dst). During the ASC phase of SC 23, there is a very weak positive correlation between CR and Dst. However, during the DSC phase of SC 23, there is a weak negative correlation. In the ASC phase of SC 24, there is a very weak negative correlation, and in the DSC phase of SC 24, there is a slightly stronger negative correlation compared to the ASC phase of SC 24. In conclusion, the ASC phase of SC 23 shows a very weak positive correlation, while the DSC phase of SC 23 shows a weak negative correlation. The ASC phase of SC 24 shows a very weak negative correlation, and the DSC phase of SC 24 shows a slightly stronger negative correlation.

The relationship between CR intensity and the ap index (a measure of geomagnetic activity) during the ASC and DSC phases of SCs 23 and 24 shows weak negative correlations with identical slopes. The DSC phase of SC 23 shows a stronger negative correlation, indicating a greater sensitivity to changes in ap during this phase. Overall, SC 23 shows a phase-dependent relationship between CR and ap, with a stronger negative correlation during the DSC phase. SC 24, on the other hand, exhibits a consistent weak negative correlation in both phases. We fitted a multiple linear regression to the CR and SSN, IMF, solar wind parameters and the geomagnetic indices parameters to observe their impact on CR variations during the ASC and the DSC phases of SC. A multiple regression fit to the logarithm values of the studied parameters gives:

$$\mathrm{CR} = A + A_1\mathrm{SSN} + A_2\mathrm{IMF} + A_3\mathrm{SWS} + A_4\mathrm{SWT} + A_5\mathrm{SWPD} + A_6 Kp + A_7 \lvert Dst \rvert + A_8 ap \quad (1)$$

where A represent the intercept and $A_1 - A_8$ the constant coefficients with the errors associated with each parameter. The values of $A, A_1 - A_8$ for each of the phases are given in Table 4. The intercept are similar for the phases, an indication that the baseline of CR intensity is nearly similar for SC 23 &24 (according to Faw and Sculits (2003) galactic cosmic radiation has been constant in intensity, except for short-term

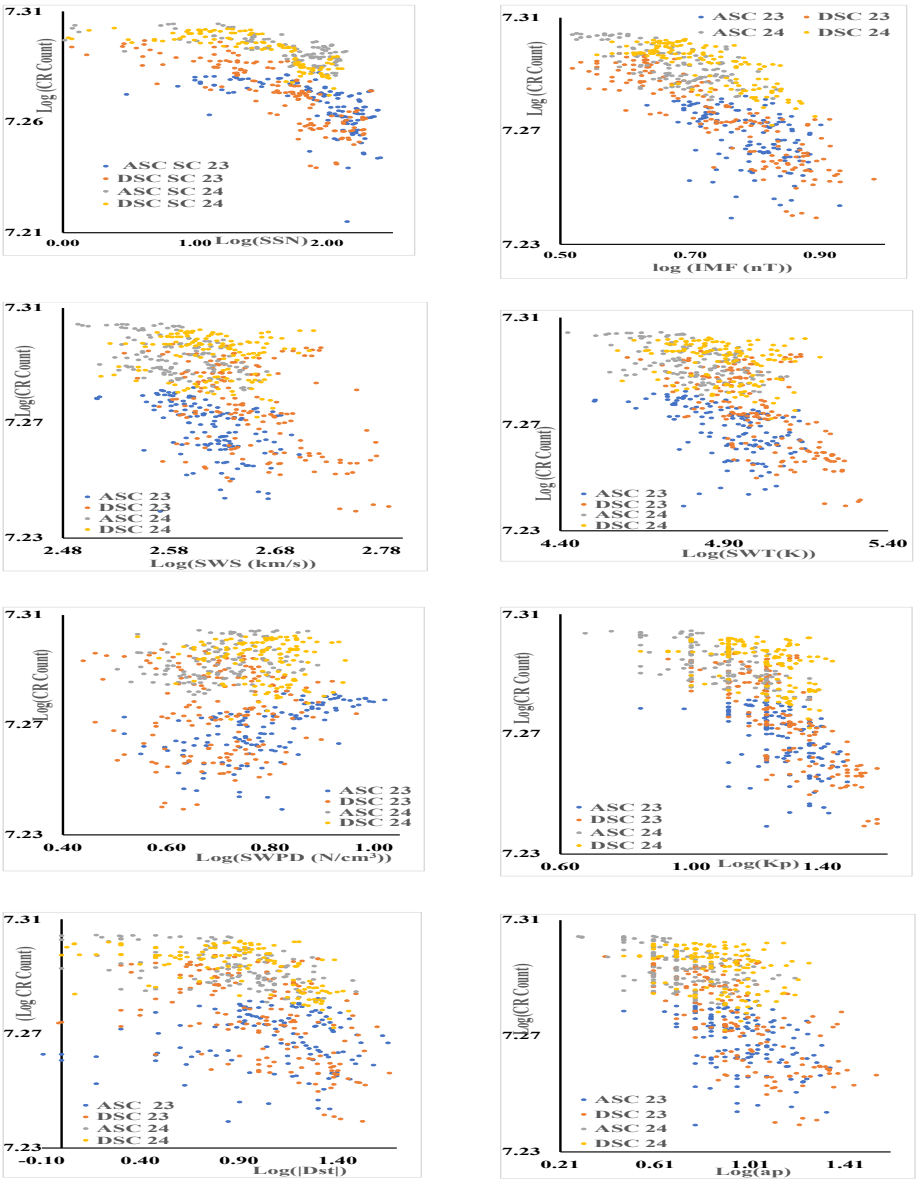

Fig. 17 log – log plots of the monthly average values of CR intensity for ASC and DSC Phases of SC 23 and 24 against the monthly average values of SSN, IMF, Solar Wind Parameters (SWS, SWT, SWPD) and Geomagnetic Activity Indices (Kp, Dst, ap)

Table 5 Multiple Regression Fit to logarithm values studied parameters

	ASC 23	DSC 23	ASC 24	DSC 24
Intercept	7.38 ± 0.11	7.30 ± 0.05	7.31 ± 0.05	7.22 ± 0.05
SSN$\times 10^{-3}$	-6.33 ± 2.64	-4.98 ± 1.54	-5.98 ± 0.93	-2.68 ± 0.98
IMF$\times 10^{-3}$	-15.80 ± 23.14	-81.42 ± 12.16	1.46 ± 10.19	-70.71 ± 11.62
SWS$\times 10^{-3}$	-18.62 ± 53.70	-8.72 ± 25.43	-14.21 ± 26.89	21.58 ± 28.54
SWT$\times 10^{-3}$	-8.15 ± 13.21	19.22 ± 10.52	9.80 ± 7.97	16.63 ± 8.85
SWPD$\times 10^{-3}$	17.57 ± 11.71	16.55 ± 6.97	-4.14 ± 5.24	7.84 ± 6.64
$Kp \times 10^{-3}$	-10.99 ± 19.24	-35.16 ± 11.65	-14.95 ± 5.04	-22.75 ± 9.15
$\lvert Dst \rvert \times 10^{-3}$	2.97 ± 2.67	5.72 ± 2.25	0.39 ± 1.41	-0.49 ± 1.56
$ap \times 10^{-3}$	0.92 ± 10.43	-1.38 ± 4.21	-0.21 ± 3.38	8.25 ± 4.84

influences of solar activity), but solar modulation is different for each phase and each SC. Hathaway and Rightmire (2010) reported differences in the behavior of the Sun's magnetic field during the ASC phase and the DSC phase, while Upton et al., (2021), reported variations in the meridional flow, which was more pronounced in Cycle 23 than in the weaker Cycle 24. These could be the sources of the differences in values and the relationships between the CR, solar wind parameters, and geomagnetic indices during different phases of SC 23 and 24 Hathaway and Rightmire (2010) noted that the transport of magnetic elements across the Sun's surface varies systematically over the SC 23 - faster at minimum and slower at maximum, account for the behaviour of the distribution at different phases of SC 23, since solar activity is related to CR intensity (e.g. Dorman and Dorman, 1967; Gupta et al., 2005)

5 Summary & Conclusion

We have conducted a study on the changes in CR intensities, solar wind parameters, and geomagnetic indices during the ascending and declining phases of SCs 23 and 24, which represent a solar magnetic cycle. Our findings indicate the following:

- Cosmic Ray (CR): CR intensity showed that during the ASC phase of SC 23, there is a higher likelihood of extreme values, unlike the declining phase, which indicates fewer outliers. The CR intensity during the ASC phase of SC 24) shows a slight tendency towards higher values and fewer extreme values. In comparison, the DSC phase of SC 24 has lower values and fewer extreme values but is more evenly spread. These results highlight differences in the monthly average CR variations between SCs 23 and 24 phases. The average values of CR intensity were higher during the declining phase than the ascending phase.
- Solar Sunspot Number (SSN): The average values of SSN are higher during ASC phases than DSC phases, but DSC phases last longer than ASC phases.
- Interplanetary Magnetic Field (IMF): The distribution is nearly similar for the ASC phases of SCs 23 and 24, and the same applies to the DSC phases, but the ASC phases are different from the DSC phases. The average value of IMF was higher during the ascending phase in SC 23, but in SC 24, the declining phase value was higher.
- Solar Wind Speed (SWS): The ascending phases were similar for both solar cycles, and the declining phases have nearly similar distributions in both cycles.

- Solar Wind Proton Density (SWPD): The distribution showed moderate right skewness during the ascending phases, but the declining phases exhibit different distribution shapes, with SC 23 being leptokurtic and SC 24 being closer to mesokurtic. The average value during SC 23 was higher during the ascending phase, but in SC 24, it was higher during the declining phase.
- Geomagnetic Parameters: The ASC phase of SC 24 shows a greater tendency towards higher values and more frequent extreme events compared to SC 23. The DSC phase of SC 23 exhibits more pronounced right skewness and higher kurtosis, indicating more extreme values.
- The correlation between CR values and the values of other parameters (SSN, IMF, SWS, SWPD, and geomagnetic indices) is similar, but the strength of the relationship differs in each phase.

The differences in solar modulation of cosmic ray flux during the ASC and DSC phases of SCs are traced to several factors including solar magnetic field strength and configuration, heliospheric current sheet tilt angle, CMEs and solar flares, and solar wind speed and density Potgieter, (2013), observed that during the ASC phase of ASC, the Sun's magnetic field becomes increasingly complex and disorganized due to the rise in solar activity. This increased complexity, along with the intensification of the solar wind, contributes to a stronger modulation of CRs, reducing their flux. During the DSC phases, solar activity wanes, and the magnetic field tends to revert to a simpler, more dipolar configuration, resulting in a weaker modulation effect, allowing more CRs to reach Earth. Heber et al., (2006), noted that the tilt angle of the heliospheric current sheet, which is the wavy surface that separates regions of the Sun's magnetic field with opposite polarities, increases during the solar maximum and the ASC phase of a cycle. This increased tilt makes it harder for CRs to penetrate the heliosphere, reducing their flux. In the DSC phase, the heliospheric current sheet tilt angle decreases, reducing its ability to deflect CRs, which leads to an increase in their flux.

Wiedenbeck et al., (2005), showed that during the ASC phase, the frequency of CMEs and solar flares is higher. These phenomena generate shock waves in the solar wind that can further scatter and block CRs, leading to a reduction in CR flux. In the DSC phase, the frequency of these events decreases, allowing more CRs to reach the inner solar system. According to Badruddin et al., (2007), the speed and density of the solar wind vary across the SC, with higher speeds and densities during the ASC phase. This increased solar wind pressure during solar maxima further shields the solar system from galactic cosmic rays. In contrast, during the DSC phase, the solar wind becomes less intense, allowing more cosmic rays to penetrate the heliosphere. This contrasted with our results since the median SWS values were higher during the DSC phases than ASC phases for SC 23 and 24, while the median value of SWPD was higher in ASC 23, lower in DSC 23, but higher in DSC 24 than ASC 24 (see Table 1). This implies the complexity of the phases of SC. These factors work in concert to modulate cosmic ray flux differently during the ASC and DSC phases of SCs, reflecting changes in solar activity and the structure of the heliosphere. In conclusion. we analysed the CR intensity variations during the ASC and the DSC phases of SC 23 and 24, our result indicates that CR intensities are modulated in varying degrees during different

phases of the solar cycle, and also the modulation is distinct from one solar circle to another.

References

Abe, K., Fuke, H., Haino, S., Hams, T., Hasegawa, M., Horikoshi, A., Itazaki, A., Kim, K. C., Kumazawa, T., Kusumoto, A., Lee, M. H., Makida, Y., Matsuda, S., Matsukawa, Y., Matsumoto, K., Mitchell, J. W., Myers, Z., Nishimura, J., Nozaki, M., Orito, R., et al., (2016). The Astrophysical Journal 822(2), 65-81

[1] [1] Abramowski, A., et al. (HESS Collaboration). (2016) Nature. 531 (7595): 476-479 doi:10.1038/nature17147.

[2] Ackermann, M. Ajello, M., Allafort, A., Baldini, L., Ballet, J., Barbiellini, G., Baring, M. G., Bastieri, D., Bechtol, K., Bellazzini, R., Blandford, R. D., Bloom, E. D., Bonamente, E., Borgland, A. W., Bottacini, E., Brandt, T. J., Bregeon, J., Brigida, M., Bruel, P., Buehler, R., et al., (2013), Science, 339(6121), 807-811, 10.1126/science.1231160.

[3] Adriani,O., Barbarino,G. C., Bazilevskaya,G. A., Bellotti, R., Boezio, M., Bogomolov, E. A., Bonechi, L., Bongi, M., Bonvicini, V., Borisov, S., Bottai, S. Bruno, A., Cafagna, F., Campana, D., Carbone, R., Carlson, P., Casolino, M., Castellini, G., Consiglio, L., De Pascale, M. P. De Santis, C., De Simone, N., Di Felice, V., Galper, A. M., Gillard, L. Grishantseva, W., Jerse, G., Karelin, A. V., Koldashov, S. V., Krutkov, S. Y., Kvashnin, A. N.,Leonov, A., Malakhov, V., Malvezzi, V., Marcelli, L., Mayorov, A. G., Menn, W., Mikhailov, V. V., Mocchiutti, E., Monaco, A., Mori, N., Nikonov, N., Osteria, G., Palma, F., Papini, P., ,et al., (PAMELA), (2011), Science 332(6025), 69-72, DOI: 10.1126/science.1199172

[4] Agrawal S.P., Shrivastava, P.K. and Shukla R.P., (1993), Proc. 23rd Int. Cosmic Ray Conf. 3:590,

[5] Aguilar, M., et al., (AMS), (2015a), Phys. Rev. Lett. 114, 171103.

[6] Aguilar, M., et al., (AMS), (2015b), Phys. Rev. Lett. 115, 21, 211101.

[7] Aharonian, F., et al., (H.E.S.S.), (2007). Phys. Rev. D75, 042004

[8] Ahluwalia, H. S., & Ygbuhay, R. C. (2014). Journal of Atmospheric and Solar-Terrestrial Physics, 113, 23-27

[9] Anchordoqui, L., Paul, T., Reucroft, S., Swain, J. (2003), International Journal of Modern Physics A. 18 (13): 222 2366. doi:10.1142/S0217751X03013879..

[10] Archer, A. et al., (VERITAS), (2018), Phys. Rev. D98, 2, 022009.

[11] Aslam, O. P. M., & Badruddin (2012). Solar Physics, 279(1), 269-286.

[12] Aslam, O. P. M., & Badruddin (2015). Journal of Geophysical Research: Space Physics, 120(2), 1081-1094

[13] Auger, P., Ehrenfest, P., Maze, R., Daudin, J. and Robley A. F., (1939), Rev. Mod. Phys 11 (3-4): 288-291, doi:10.1103/RevModPhys.11.288.

[14] Ave, M., Boyle, P. J., Gahbauer, F., Hoppner, C., Hörandel, J. R., Ichimura, M., Müller, D., and Romero-Wolf, A., (2008). Astrophysical Journal, 678, 262, DOI 10.1086/529424

[15] Badruddin, M., Yadav, R. S., & Yadav, N. R. (2007). Cosmic ray intensity variations during solar cycle phases: A study of long-term changes. Journal of Atmospheric and Solar-Terrestrial Physics, 69(6), 601-611. https://doi.org/10.1016/j.jastp.2006.11.013

[16] Balasubrahmanyan, V. K. (1969).Solar Physics 7, 39-45, https://doi.org/10.1007/BF00148403,

[17] Balogh, A., Hudson, H.S., Petrovay, K., et al. (2014), Space Sci Rev 186, 1–15. doi.org/10.1007/s11214-014-0125-8

[18] Barichello, J.C., (1978), Solar-Terrestrial Relations? M.Sc. Thesis, Univ. Of Calgary, Canada.

[19] Belov, A., Eroshenko, E., Yanke, V., Oleneva, V., Abunin, A., Abunina, M., Papaioannou, A., Mavromichalaki, H. (2018), Solar Physics 293, 68

[20] Bhattacharya R., Roy M., IJEST, vol. 6, 24 2014.

[21] Blasi, P.; Epstein, R. I.; Olinto, A. V. (2000). The Astrophysical Journal. 533 (2), L123, L126. doi:10.1086/312626.

[22] Blazquez-García, A., Conde, A., Mori, U., Lozano, J. A., (2021), ACM Computing Surveys 54(3):1-33, DOI: 10.1145/3444690Solanki, 2002

[23] Castellina, A., Donato, F., In Oswalt, T.D.; McLean, I.S.; Bond, H.E.; French, L.; Kalas, P., (2012), Barstow, M.; Gilmore, G.F.; Keel, W. (eds.). Planets, Stars, and Stellar Systems (1 ed.). Springer. ISBN 978-90-481-8817-8.

[24] Chaurasiya, D. K., Goyal, S., Shrivastava, K., Gupta, R. S., IJIRSET, Vol 17, issue 7, 2023 e-ISSN2319-8753, DOI:10.15680/IJIRSET.2023.1207125. (2023)

[25] Cliver. E.W. & Ling, A.G. (2001), Astrophys. J, 551 L189-L192.

[26] Conway A. J., (1998), New Astronomy Reviews., 42(5):343-394.

[27] Denkmayr K., Cugnon P., (1997), Proceedings of the 5th Solar-Terrestrial Predictions Workshop. In R. Heckman, editor. Japan: Communications Research

Laboratory. p. 103.

[28] Dorman, I. V. and Dorman, L. I. (1967). J. Geophys. Res., 72, 1513. Doi. 10.1029/JZ072i005p01513

[29] Dumbovic, M., Vrsnak, B., Calogovic, J., Karlica, M., (2011), Astronomy and Astrophysics 531(A91), 1

[30] Echer, E., Lucas, A.d., Hajra, R. et al. (2023), Braz J Phys 53, 79. doi.org/10.1007/s13538-023-01294-w

[31] Echer, E., Rigozo N. R., Souza M. P., et al. (2004), Annales Geophysicae. 22:2239-2243,

[32] Faw, R. E., and Shultis, J. K., (2003), in Encyclopaedia of Physical Science and Technology (Third Edition) ed R. A. Meyers,

[33] Fisher, R.A. (1915), Biometrika 10(4), 507

[34] Forbush, S.E., (1946), Phys. Rev. 70, 771.

[35] Gieseler, J., Heber, B., & Herbst, K. (2017). Journal of Geophysical Research: Space Physics, 122(10), 10964-10979

[36] Gonzalez, W. D., Echer, E., Tsurutani, B. T., & Gonzalez, A. L. C. (2011). Interplanetary Origin of Intense, Superintense, and Extreme Geomagnetic Storms. Space Science Reviews, 158(1), 69-89. doi.org/10.1007/s11214-010-9715-2).

[37] Gopalswamy, N., Yashiro1, S., Mäkelä1, P., Michalek, G., Shibasaki, K., and Hathaway, D. H. (2012), The American Astronomical Society. The Astrophysical Journal Letters, 750(2) doi: 10.1088/2041-8205/750/2/L42

[38] Gopalswamy, N., et al. (2015). The Astrophysical Journal Letters, 804(1), L23. doi.org/10.1088/2041-8205/804/1/L23).

[39] Gupta, M., Mishra, V. K. and Mishra, (2005), 29th International Cosmic Ray Conference Pune 2, 147-150,

[40] Hanslmeier A., Denkmayr K., Weiss P., (1999), Solar Physics. 184(1):213-218.

[41] Hathaway, D. H. & Upton, L. (2014), Journal of Geophysical Research: Space Physics, doi.org/10.1002/2013JA019432

[42] Hathaway, D. H. and Rightmire, L. (2010), American Astronomical Society, AAS Meeting No. 216, id.319.02; Bulletin of the American Astronomical Society, Vol. 41, p.909.

[43] Heber, B., Fichtner, H., & Scherer, K. (2006). Solar and heliospheric modulation of galactic cosmic rays. Space Science Reviews, 125(1-4), 81-93. https://doi.org/10.1007/s11214-006-9048-7

[44] Heber, B., Kopp, A., Gieseler, J., Mewaldt, R. A., Möbius, E., & Rice, J. (2009). Modulation of galactic cosmic ray protons and electrons during the unusual solar minimum of 2006 to 2009. The Astrophysical Journal, 699(2), 1956.

[45] Hjorth, J., Bloom, J. S., (2012), In C. Kouveliotou; R. A. M. J. Wijers; S. E. Woosley (eds.). Gamma-Ray Bursts. Cambridge Astrophysics Series. Vol. 51. Cambridge University Press. pp. 169-190..

[46] Hoyt, D. V., Schatten, K. H., (1998) Solar Physics. 179(1):189-219.

[47] Hoyt, D. V., Schatten, K. H.,. (1979), USA: Oxford University Press;

[48] Iwok, I.A.: 2011, Amer. J. Sci. Ind. Res. 2, 488. American Journal Of Scientific And Industrial Research 2011, Science Huβ, doi:10.5251/ajsir.2011.2.4.488.490

[49] Jolliffe, I. T., & Stephenson, D. B. (2012). Forecast Verification: A Practitioner's Guide in Atmospheric Science. Wiley Publishers

[50] Jothe, M. K., Singh, M., Shrivastava, P. K., (2010), Ind. J. Sci. Res. 1, 55

[51] Kane R. P. (2006), Advances in Space Research. 37:1261-1264.

[52] Kass, R. E., Eden, U. T., & Brown, E. N. (2018). Smoothing and inference for time series data. Journal of Time Series Analysis.

[53] Kilpua, E. K. J., Hietala, H., Koskinen, H. E. J., Fontaine, D., & Turc, L. (2015). Journal of Space Weather and Space Climate, 5, A29. doi.org/10.1051/swsc/2015027).

[54] Kuwabara, T., Munakata, K., Yasue, S., Kato, C., Akahane, S., Fujimoto, K., ... & Bieber, J. W. (2009). Journal of Geophysical Research: Space Physics, 114(A5)

[55] Layden A. C., Fox P. A., Howard J. M., et al., (1991), Solar Physics. 132(1):1-40.

[56] Lingri, D., Mavromichalaki, H., Belov, A., Eroshenko, E., Yanke, V.G., Abunin, A., Abunina, M., (2016), Solar Physics 297, 1

[57] Mann, M. E., et al. (2008). Geophysical Research Letters, 35(16), doi.org/10.1029/2008GL034716

[58] Mavromichalaki, H., Papaioannou, A., Plainaki, C., Sarlanis, C., Souvatzolou, G., Gerontidou, M., Papailiou, M., Eroshenko, E., Belov, A., et al., (2011), Advances in Space Research, 47(12), 2210-2222, doi.10.1016/j.asr.2010.02.019

[59] Mavromichalaki, H., Vassilaki, A., and Marmatsouri, E., (1998) Solar Physics 115, 345,

[60] McComas, D. J., et al. (2013) Weakest Solar Wind of the Space Age and the Current 'Mini' Solar Maximum. The Astrophysical Journal, 779(1), 2. doi.org/10.1088/0004-637X/779/1/2

[61] Mishra, W., Sahani P. S., Khuntia, S., Chakrabarty D., (2024), Distribution and recovery phase of geomagnetic storms during solar cycles 23 and 24, Monthly Notices of the Royal Astronomical Society, 530(3), 3171–3182, doi.org/10.1093/mnras/stae1045

[62] Mishra, M.P., (2005), 29th International Cosmic Ray Conference Pune 2, 159-162,

[63] Mishra, V.K., Mishra, A.P. (2016), Indian J Phys 90, 1333-1339, https://doi.org/10.1007/s12648-016-0895-9,

[64] Moraal, H., & McCracken, K. G. (2012). Space Science Reviews, 176(1-4), 299-319.

[65] Okike, O., Alhassan, J.A., Iyida, E.U., Chukwude, A.E., (2021), Monthly Notices of the Royal Astronomical Society 503, 5675

[66] Okike, O., Nwuzor, O.C., Odo, F.C., Iyida, E.U., Ekpe, J.E., Chukwude, A.E., (2020), MNRAS,

[67] Okike, O., Umahi, A.E., (2019), Solar Physics 294(2)

[68] Onuchukwu C. C. (2018), Phys Astron Int J., 2(4):300-308

[69] Persai, S. K., Jothe, M. K., Singh, M., K Shrivastava, (2015), International Journal of Science and Research (IJSR) Volume 4 Issue 12,

[70] Potgieter, M. S. (2013). Living Reviews in Solar Physics, 10(1), 3. doi.org/10.12942/lrsp-2013-3.

[71] Potgieter, M. S. (2013). Solar modulation of cosmic rays, Living Reviews in Solar Physics, 10(3), 1-53. https://doi.org/10.12942/lrsp-2013-3

[72] Ramesh K. B. (2010), The Astrophysical Journal Letters.;712(1):L77–L80

[73] Rangarajan, G.K., Lyemori, T., (1997), Annales Geophysicae 15, 1271–1290. doi.org/10.1007/s00585-997-1271-z

[74] Rees, M., Sargent, W. (1968), Nature 219, 1005–1009. doi.org/10.1038/2191005a0

[75] Richardson, I. G. (2013). Living Reviews in Solar Physics, 10(1), 3. doi.org/10.12942/lrsp-2013-1).

[76] Rudebusch, G. D., & Williams, J. C. (2009). Journal of Business & Economic Statistics, 27(4), 492-503

[77] Ruzmaikin, A. (2001), Space Science Reviews 95, 43–53. doi.org/10.1023/A:1005290116078

[78] Sharma, S., (2008), Atomic and Nuclear Physics. Pearson Education India. p. 478. ISBN 978-81-317-1924-4..

[79] Simpson, J. A., (1983)Annual Review of Nuclear and Particle Science, vol. 33, 323 382 10.1146/annurev.ns.33.120183.001543

[80] Simpson, J. A., (1990), Proc. Int. Cosmic Ray Conf. 12, 187.

[81] Singh, A., Chaudhari, A., Sharma, G., and Singh, A. K., (2024), Research in Astronomy and Astrophysics, 24(2), doi.10.1088/1674-4527/ad1922

[82] Singh, S., Palb, M., Kumar, P., Ranic, A., Thakur, N., Singhd, K., Mishrae, A. P. (2023), 38th International Cosmic Ray Conference (ICRC2023),

[83] Solanki, S. (2002), Astronomy & Geophysics, 43(5), 9-13, doi.org/10.1046/j.1468-4004.2002.43509.x

[84] Solanki, S. (2003),. The Astron Astrophys Rev 11, 153–286. doi.org/10.1007/s00159-003-0018-4

[85] Sparvoli, R., and Martucci, M., (2022), Applied Sciences 2022, 12(7), 3459; doi.org/10.3390/app12073459

[86] Spiegel E. A. (1994), In Lectures on Solar and Planetary Dynamos. In: Proctor MRE, Gilbert AD, editors. UK: Cambridge University Press, 245.

[87] Tsurutani, B. T., Echer, E., Gonzalez, W. D., & Guarnieri, F. L. (2014).. Journal of Geophysical Research: Space Physics, 119 (5), 3716-3719. doi.org/10.1002/2014JA019805).

[88] Tukey, J. W. (1977). Exploratory Data Analysis. Addison-Wesley Publishing Company Reading, Mass. Menlo Park, Cal., London, Amsterdam, Don Mills, Ontario, Sydney XVI, 688 S.

[89] Upton, L., Hathaway, D. H., Sushant, M., (2021), AGU Fall Meeting 2021, held in New Orleans, LA, 13-17 December 2021, id. SH54A-012021AGUFMSH54A..01U

[90] Usoskin, I. G., Huotari, K. A., Kovaltsov, G. A., and Mursula, K. (2005). Journal of Geophysical Research vol. 110, A108, doi: 10, 1029/005 JA 011250,

[91] Usoskin, I. G., Mursula, K.,& Kovaltsov, G. A. (2002).. Advances in Space Research, 29(3), 397-404. doi.org/10.1016/S0273-1177(02)00097-3).

[92] Vaclav, C., (2009), Vol. I. Eolss Publishers. p. 165. ISBN 978-1-84826-104-4.

[93] van Allen, J.A., (2000), Geophys. Res. Lett, 27, 2453-2456.

[94] Vannoni, G.; Aharonian, F. A.; Gabici, S.; Kelner, S. R.; Prosekin, A. (2011), Astronomy & Astrophysics. 536: A56. doi:10.1051/0004-6361/200913568.

[95] White, O., Kopp, G., Snow, M., et al. (2011),. Solar Physics 274, 159-162. doi.org/10.1007/s11207-010-9680-7

[96] Wiedenbeck, M. E., Cohen, C. M., Cummings, A. C., Leske, R. A., Stone, E. C., & von Rosenvinge, T. T. (2005). Observations of solar energetic particles from large CMEs in solar cycles 23 and 24. Astrophysical Journal Letters, 633(1), L103-L106. https://doi.org/10.1086/497631

[97] Xu T., Wu J, Wu Z., et al., (2008), Chinese Journal of Astronomy and Astrophysics. 8(3)337-342.

[98] Zhan L. S., Zhao H. J., Liang H. F., (2003), New Astronomy, 8, 449-456.

[99] Zhang, J., Temmer, M., Gopalswamy, N., et al. (2021). Prog Earth Planet Sci 8, 56 doi.org/10.1186/s40645-021-00426-7

[100] Zweibel, E. G. (2013), Phys. Plasmas 20 (5), 055501 doi.org/10.1063/1.4807033

[101] http://www.cosmicrays.unam.mx/.

[102] http://www.nmdb.eu,

[103] http://www.sidc.be/SILSO/.